Monthly Notices
of the
ROYAL ASTRONOMICAL SOCIETY

Mon. Not. R. Astron. Soc. **412,** 1823–1827 (2011) doi:10.1111/j.1365-2966.2010.18020.x

Radiative parameters of Nb I excited states

G. Malcheva,[1] H. Nilsson,[2] L. Engström,[3] H. Lundberg,[3] É. Biémont,[4,5] P. Palmeri,[5] P. Quinet[4,5] and K. Blagoev[1]⋆

[1]*Institute of Solid State Physics 'Acad. G. Nadjakov', Bulgarian Academy of Sciences, 72 TzarigradskoChaussee, BG – 1784 Sofia, Bulgaria*
[2]*Lund Observatory, Lund University, PO Box 43, S-221 00 Lund, Sweden*
[3]*Department of Physics, Lund University, PO Box 118, S-221 00 Lund, Sweden*
[4]*IPNAS (Bât. B15), University of Liège, SartTilman, B-4000 Liège, Belgium*
[5]*Astrophysics and Spectroscopy, University of Mons-UMONS, B-7000 Mons, Belgium*

Accepted 2010 November 11. Received 2010 November 11; in original form 2010 September 29

ABSTRACT

Radiative lifetimes of 17 excited levels of Nb I, in the energy range 27 400–47 700 cm^{-1} (5p y $^6D^\circ_{9/2}$, 5p x $^6D^\circ_{7/2}$, 5p w $^4G^\circ_{7/2,9/2,11/2}$, 5s5p v $^4D^\circ_{1/2,3/2,5/2,7/2}$, 5s6p n $^4D^\circ_{1/2,3/2,5/2,7/2}$, 5s6p o $^4F^\circ_{3/2,5/2,7/2,9/2}$), have been measured. For 15 of these levels, the lifetimes are obtained for the first time. The lifetimes were measured using the time-resolved laser-induced fluorescence technique and the experiments are complemented by a theoretical investigation using a relativistic Hartree–Fock method including core polarization. By combining the experimental lifetimes and the calculated branching fractions, we obtain transition probabilities for the individual de-excitation channels from the investigated levels.

Key words: atomic data – atomic processes – methods: laboratory.

1 INTRODUCTION

Radiative parameters of atoms and ions are generally important data for plasma physics and astrophysics. Niobium is of particular interest, since it is a highly refractory metal that can be included in the inner walls of fusion devices. In addition, niobium has been observed in heavy-element stars, like the M-type long-period variable (LPV) o Ceti (Mira) and MS-type LPV, χ Cyg (Wallerstein & Dominy 1986). In this paper, Nb I spectra have been investigated to derive the abundance of niobium in these stars.

In a recent investigation (Nilsson et al. 2010), transition probabilities for astrophysically interesting spectral lines of Nb II and Nb III were derived by combining lifetimes measured by the time-resolved laser-induced fluorescence technique (TR-LIF), branching fractions from spectra recorded using Fourier transform spectroscopy and theoretical calculations using a relativistic Hartree–Fock method. The results obtained were used to determine the niobium abundance in the Sun and metal-poor stars rich in neutron-capture elements. This work continues the investigation of radiative properties of niobium, particularly for highly excited states in Nb I.

There are only three papers in the literature reporting on radiative lifetimes of Nb I. The first investigation was performed by Duquette & Lawler (1982). These authors used a novel source for highly refractory elements based on a hollow-cathode atomic beam combined with TR-LIF. The radiative lifetimes of a number of odd levels, with energies between 19 900 and 27 300 cm^{-1}, are reported in this paper. In Rudolph & Helbig (1982), radiative lifetimes of six levels (y $^4F^\circ_{9/2,11/2}$; x $^6D^\circ_{3/2,5/2,7/2}$; y $^6D^\circ_{9/2}$) in Nb I are reported. These measurements were made by TR-LIF on an atomic beam produced by a double cage made of tungsten and niobium wires. The results were compared with the arc measurements of Corliss & Bozman (1962). Furthermore, radiative lifetimes of 11 levels in Nb I have been measured in Kwiatkowski et al. (1982), again using TR-LIF. The investigated levels belong to the following terms: z $^4F^\circ$, y $^6F^\circ$, y $^6D^\circ$ and x $^6D^\circ$, and the energy levels are in the range 23 570–27 430 cm^{-1}. The lifetime values reported in Kwiatkowski et al. (1982) were used to obtain oscillator strengths for some spectral lines of solar interest. Absolute transition probabilities of Nb I spectral lines, emitted from levels with energies in the interval 19 624–27 975 cm^{-1}, were determined by Duquette et al. (1986). It should be emphasized that, in all these papers, only low-lying levels of Nb I have been investigated.

In this work, we extend the previous investigations and report on radiative lifetimes of 15 high-lying odd-parity states of Nb I in the energy range 27 415–47 680 cm^{-1}. In parallel with the measurements, we have performed theoretical calculations of branching fractions for the various transitions depopulating the investigated levels using a multiconfiguration Hartree–Fock method with explicit treatment of core-polarization effects.

2 EXPERIMENT

According to Moore's tables of atomic energy levels (Moore 1958), the ground state of neutral niobium is [Kr] $4d^45s$ a $^6D_{1/2}$ with the close-lying metastable $4d^35s^2$ a ^4F term only 1000–3000 cm^{-1} away. The latter term has been the starting point in our excitation schemes as shown in Fig. 1 and Table 1.

⋆E-mail: kblagoev@issp.bas.bg

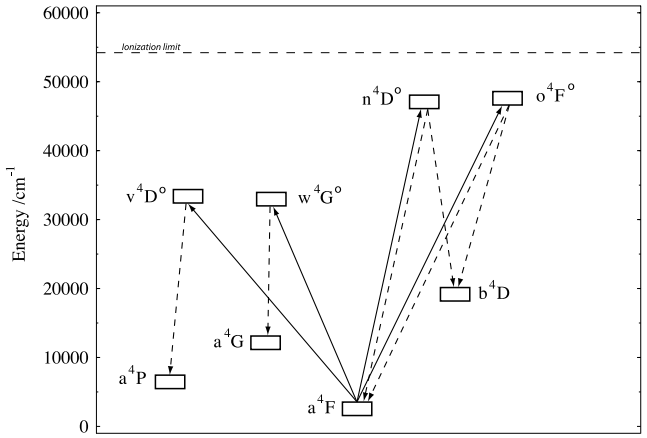

Figure 1. Partial energy level diagram of Nb I. Only the levels involved in the experiment are shown. All upper levels are pumped from the metastable $4d^3\,5s^2\,a^4F$ term, as indicated by the solid arrows. The observed fluorescence channels are shown as dashed lines.

Table 1. Odd Nb I levels measured in the present experiment and the corresponding excitation schemes.

Level[a]	E^a (cm^{-1})	Excitation[b] (λ_{air}/nm)	Excitation schemes[c]	Detection (λ_{air}/nm)
$4d^3 5s5p$ y $^6D_{9/2}$	27 419.62	374.08	2ω+S	379
$4d^4 5p$ x $^6D_{7/2}$	27 427.07	373.97	2ω+S	374
$4d^4 5p$ w $^4G_{7/2}$	32 501.33	323.23	2ω	493
$^4G_{9/2}$	32 802.44	326.18	2ω	491
$^4G_{11/2}$	33 428.20	326.46	2ω	479
$4d^3 5s5p$ v $^4D_{1/2}$	33 011.45	313.69	2ω	357
$^4D_{3/2}$	33 717.01	311.14	2ω	348
$^4D_{5/2}$	33 872.18	315.18	2ω	350
$^4D_{7/2}$	34 168.94	318.75	2ω	354
$4d^3 5s5p$ n $^4D_{1/2}$	45 978.84	222.96	3ω	307
$^4D_{3/2}$	46 364.79	221.06	3ω	304
$^4D_{5/2}$	46 812.58	218.89	3ω	312
$^4D_{7/2}$	47 275.64	218.80	3ω	224
$4d^3 5s5p$ o $^4F_{3/2}$	46 170.04	222.01	3ω	306
$^4F_{5/2}$	46 543.56	220.19	3ω	316
$^4F_{7/2}$	47 022.78	220.22	3ω	223
$^4F_{9/2}$	47 680.59	219.58	3ω	222

[a]Moore (1958).
[b]All levels are pumped from the metastable $4d^3 5s^2$ a ^{4}F term as shown in Fig. 1.
[c]2ω and 3ω mean the second and third harmonic, and S means the first Stokes component of the Raman scattering.

The TR-LIF method was used to measure the radiative lifetimes of excited niobium states. The experimental set-up has previously been described in detail in Bergström et al. (1988) and also in a recent investigation of lifetimes in Nb^+ and Nb^{2+} (Nilsson et al. 2010), and only a short description will be given below.

Free niobium atoms were created in a laser-produced plasma by focusing a 10-Hz-frequency doubled Nd:YAG laser on to a rotating target, placed inside a vacuum chamber with a pressure of 10^{-5} mbar. The atoms were then selectively excited by crossing the ablation plasma 1 cm above the target with the light emitted from a dye laser, using DCM dye, which was pumped by an Nd:YAG laser. The pump laser pulses were temporally reduced in a compressor based on stimulated Brillouin scattering in water and the final excitation pulses had a duration of about 1.5 ns. The wavelengths necessary to excite the different states investigated were obtained by frequency doubling and tripling in KDP and BBO crystals. To cover a broader wavelength range, a Raman shifter, based on scattering in hydrogen gas, was used to give Stokes components of 4153 cm^{-1}. The two Nd:YAG lasers were synchronized by a pulse generator, which provided a temporal delay between ablation and excitation pulses. The wavelengths and excitation schemes used are presented in Table 1.

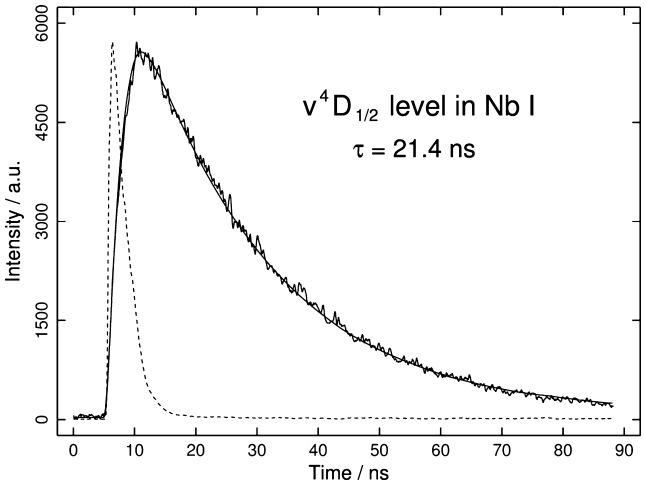

Figure 2. Decay of the level v $^4D_{1/2}$at 33 011 cm^{-1}, with an evaluated lifetime of 21.4 ± 1.5 ns. Background subtracted data points are plotted together with the fitted single exponential convolved by the measured laser pulse (solid line). The dashed curve shows the recorded laser pulse.

The spectral lines of interest from the LIF signal were selected by a 1/8-m grating monochromator with its entrance slit oriented parallel to the excitation laser beam. The signal was registered by a fast micro-channel-plate photomultiplier tube (Hamamatsu R3809U) and digitized by a Tektronix DPO 7254 oscilloscope. The decay curves were formed by averaging over 1000 laser excitation pulses and then transferred to a PC together with a measurement of the excitation laser pulse from a fast photodiode. The code DECFIT was then used to extract the experimental lifetimes from a least-squares fit of a single exponential decay deconvolved by the recorded laser pulse shape.

The influence of radiation trapping and/or collisional quenching was investigated by varying the delay between the ablation and excitation pulses, thus producing measurements with different concentrations of atoms in the ground electronic configuration. The typical delay used was in the interval 2–7 μs. The possible effect of saturation of the laser pulses was checked and avoided by inserting neutral density filters in the excitation laser beam. A typical decay curve for the v $^4D_{1/2}$ level is presented in Fig. 2.

3 CALCULATIONS

The pseudo-relativistic Hartree–Fock (HFR) method developed by Cowan (1981) and adapted for taking core-polarization effects into account (see e.g. Quinet et al. 1999) has been used in this work. 10 even and nine odd-parity electronic configurations were explicitly included in the physical model, that is, $4d^5 + 4d^4 5s + 4d^4 6s + 4d^4 5d + 4d^3 5s^2 + 4d^3 5p^2 + 4d^3 5d^2 + 4d^3 5s5d + 4d^3 5s6s + 4d^2 5s5p^2$ and $4d^4 5p + 4d^4 6p + 4d^4 4f + 4d^4 5f + 4d^3 5s5p + 4d^3 5s6p + 4d^3 5p5d + 4d^2 5s^2 5p + 4d^2 5p^3$, respectively. The dipole polarizability used in the core-polarization potential was the one

computed by Fraga et al. (1976) for an Nb IV ionic core, that is, $\alpha_d = 5.80a_0^3$, while the cut-off radius was chosen to be equal to the HFR mean value $\langle r \rangle$ of the outermost core orbital (4d), that is, $r_c = 1.96a_0$. To reduce as much as possible the differences between the experimental and theoretical energy levels, a well-established semi-empirical fitting procedure (Cowan 1981) was applied to the radial parameters characterizing the $4d^5$, $4d^45s$, $4d^35s^2$, $4d^45p$ and $4d^35s5p$ configurations. This optimization process was performed using the available experimental energy levels listed in the NIST compilation (Moore 1958) recently revised and extended by Kröger et al. (2004, 2007). In this fitting procedure, the high odd energy levels available (above 38 000 cm^{-1}) were not considered, because many of them were found to be strongly mixed with levels belonging to experimentally unknown configurations, such as $4d^46p$, $4d^35s6p$, $4d^25s^25p$, etc., as illustrated in Fig. 3. This strong mixing is such that, according to our calculations, about one-third of the levels in the range 38 000–45 000 cm^{-1} have a leading component belonging to $4d^46p$, $4d^35s6p$ or $4d^25s^25p$ with average purities of 67, 38 and 25 per cent, respectively, while the average purities of $4d^45p$ and $4d^35s5p$ levels are found to be about 25 per cent in the same energy region. Consequently, an unambiguous connection between experimental and calculated level values could not be established even when using the experimental values available for the Landé factors.

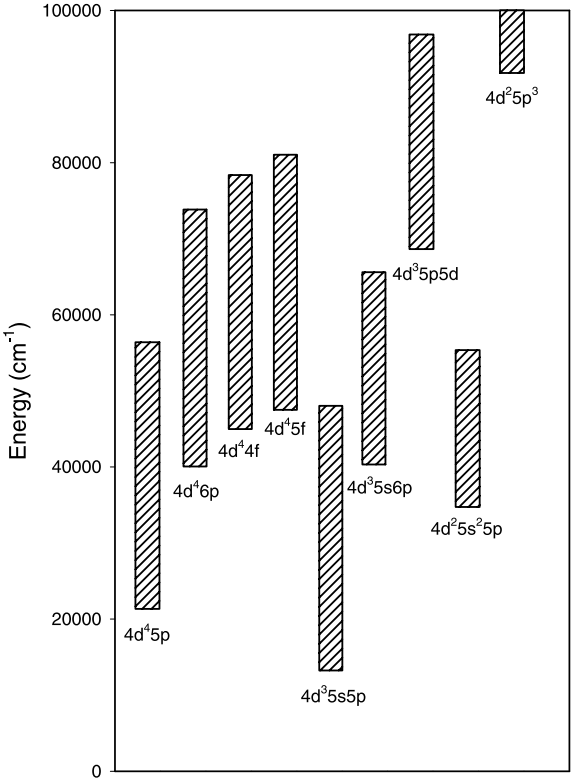

Figure 3. Energies for odd-parity configurations of Nb I as predicted by *ab initio* HFR calculations.

4 RESULTS AND DISCUSSION

The lifetimes obtained in this work are presented in Table 2 and represent the averages of at least 10 different measurements performed under slightly different experimental conditions. The uncertainties quoted include statistical errors from the fitting procedure as well as the variation in the results between different measurements. As an overall test, we also include two levels, with lifetimes that are typical of those found in this work, that have been measured by several groups previously. As seen in Table 2, there is good agreement between the two sets of data.

For the $4d^45p$ and $4d^35s5p$ levels, our calculated lifetimes are also reported in Table 2. The latter values are found to be in good agreement with the measurements, if we exclude the w $^4G_{11/2}$ level for which the calculation inexplicably gives a radiative lifetime a factor of 2 longer than the experimental value. In Table 3, transition probabilities deduced from the combination of the experimental lifetimes and the calculated branching fractions obtained in this work are reported. Only transitions with *gA*-values greater than 10^7 s^{-1} are given in this table. These new radiative data for 41 Nb I lines covering the spectral region 306–570 nm constitute an extension of the

Table 2. Experimental and theoretical lifetimes (τ in ns) in Nb I.

Level	E_{exp} (cm^{-1})	g_{exp}	E_{calc} (cm^{-1})	g_{calc}	Experimental (this work)	Experimental (other authors)	Theoretical (this work)
x $^6D_{7/2}$	27 427.07				8.1 ± 0.4	7.9(6)[3], 7.7(4)[2], 7.9(4)[5]	9.4
y $^6D_{9/2}$	27 419.62				15.0 ± 0.7	14.7(1.0)[3], 15.1(8)[2]	13.9
w $^4G_{7/2}$	32 501.33	1.060	32 712	1.126	28.5 ± 2.0		32.5
w $^4G_{9/2}$	32 802.44	1.210	32 810	1.197	41.1 ± 3.0		47.0
w $^4G_{11/2}$	33 428.20	1.270	33 322	1.268	38.2 ± 3.0		60.6
v $^4D_{1/2}$	33 011.45	0.460	32 665	0.378	21.4 ± 1.5		16.1
v $^4D_{3/2}$	33 717.01	1.230	33 464	1.205	14.6 ± 1.0		15.5
v $^4D_{5/2}$	33 872.18	1.350	33 644	1.308	11.4 ± 0.6		11.7
v $^4D_{7/2}$	34 168.94	1.390	33 969	1.418	10.1 ± 0.6		8.2
n $^4D_{1/2}$	45 978.84				6.5 ± 0.3		
n $^4D_{3/2}$	46 364.79				6.7 ± 0.3		
n $^4D_{5/2}$	46 812.58				6.9 ± 0.3		
n $^4D_{7/2}$	47 275.64				8.4 ± 0.4		
o $^4F_{3/2}$	46 170.04				6.0 ± 0.3		
o $^4F_{5/2}$	46 543.56				4.7 ± 0.3		
o $^4F_{7/2}$	47 022.78				6.9 ± 0.3		
o $^4F_{9/2}$	47 680.59				7.0 ± 0.3		

Table 3. Measured lifetimes (τ, in ns), calculated branching fractions (BF_{HFR}) and transition probabilities (gA) in Nb I. Only transitions with $gA > 10^7\ s^{-1}$ are given in the table.

Upper level	Lower level		λ_{air} (nm)	BF_{HFR}	gA^a ($10^7\ s^{-1}$)
	Designation	E_{exp} (cm^{-1})			
$4d^45p\ w\ {}^4G^\circ_{7/2}$	$4d^35s^2\ a\ {}^4F_{7/2}$	2154.11	329.425	0.099	2.78
$E = 32\,501.33\ cm^{-1}$	$4d^45s\ a\ {}^4G_{5/2}$	12 018.25	488.072	0.213	5.99
$\tau = 28.5 \pm 2.0$	$4d^35s^2\ a\ {}^2H_{9/2}$	12 102.12	490.078	0.186	5.21
	$4d^45s\ b\ {}^4F_{5/2}$	12 692.12	504.675	0.168	4.72
	$4d^35s^2\ a\ {}^2F_{5/2}$	13 404.77	523.509	0.064	1.79
$4d^45p\ w\ {}^4G^\circ_{9/2}$	$4d^35s^2\ a\ {}^4F_{9/2}$	2805.36	333.270	0.098	2.38
$E = 32\,802.44\ cm^{-1}$	$4d^35s^2\ a\ {}^2G_{9/2}$	9328.88	425.891	0.049	1.18
$\tau = 41.1 \pm 3.0$	$4d^45s\ a\ {}^4H_{11/2}$	11 247.88	463.809	0.133	3.24
	$4d^45s\ a\ {}^4G_{7/2}$	12 136.86	483.761	0.272	6.62
	$4d^35s^2\ a\ {}^2H_{11/2}$	12 502.97	492.486	0.067	1.63
	$4d^45s\ b\ {}^4F_{7/2}$	12 982.38	504.399	0.127	3.09
	$4d^45s\ b\ {}^4D_{7/2}$	15 282.35	570.615	0.102	2.49
$4d^35s5p\ v\ {}^4D^\circ_{1/2}$	$4d^35s^2\ a\ {}^4F_{3/2}$	1142.79	313.697	0.260	2.43
$E = 33\,011.45\ cm^{-1}$	$4d^35s^2\ a\ {}^4P_{1/2}$	4998.17	356.872	0.487	4.55
$\tau = 21.4 \pm 1.5$					
$4d^45p\ w\ {}^4G^\circ_{11/2}$	$4d^35s^2\ a\ {}^4F_{9/2}$	2805.36	326.460	0.085	2.68
$E = 33\,428.20\ cm^{-1}$	$4d^45s\ a\ {}^4H_{13/2}$	11 524.65	456.419	0.106	3.34
$\tau = 38.2 \pm 3.0$	$4d^45s\ a\ {}^4G_{9/2}$	12 357.70	474.464	0.440	13.83
	$4d^45s\ b\ {}^4F_{9/2}$	13 145.71	492.899	0.213	6.69
$4d^35s5p\ v\ {}^4D^\circ_{3/2}$	$4d^35s^2\ a\ {}^4F_{3/2}$	1142.79	306.902	0.108	2.95
$E = 33\,717.01\ cm^{-1}$	$4d^35s^2\ a\ {}^4F_{5/2}$	1586.90	311.144	0.296	8.11
$\tau = 14.6 \pm 1.0$	$4d^35s^2\ a\ {}^4P_{1/2}$	4998.17	348.104	0.115	3.16
	$4d^35s^2\ a\ {}^4P_{3/2}$	5297.92	351.776	0.203	5.57
	$4d^45s\ b\ {}^4P_{1/2}$	13 629.15	497.674	0.039	1.07
	$4d^45s\ b\ {}^4P_{3/2}$	14 211.30	512.528	0.047	1.28
$4d^35s5p\ v\ {}^4D^\circ_{5/2}$	$4d^35s^2\ a\ {}^4F_{5/2}$	1586.90	309.649	0.111	5.85
$E = 33\,872.18\ cm^{-1}$	$4d^35s^2\ a\ {}^4F_{7/2}$	2154.11	315.186	0.173	9.10
$\tau = 11.4 \pm 0.6$	$4d^35s^2\ a\ {}^4P_{3/2}$	5297.92	349.865	0.334	17.59
	$4d^35s^2\ a\ {}^4P_{5/2}$	5965.45	358.234	0.084	4.44
	$4d^45s\ a\ {}^4D_{3/2}$	8705.32	397.236	0.026	1.36
	$4d^45s\ a\ {}^4D_{5/2}$	9043.14	402.640	0.029	1.53
	$4d^45s\ b\ {}^4F_{5/2}$	12 692.12	472.010	0.032	1.69
	$4d^45s\ b\ {}^4F_{7/2}$	12 982.38	478.569	0.027	1.43
	$4d^35s^2\ a\ {}^2F_{7/2}$	13 515.20	491.095	0.026	1.37
	$4d^45s\ b\ {}^4P_{3/2}$	14 211.30	508.482	0.040	2.11
	$4d^45s\ b\ {}^4D_{7/2}$	15 282.35	537.779	0.022	1.16
$4d^35s5p\ v\ {}^4D^\circ_{7/2}$	$4d^35s^2\ a\ {}^4F_{7/2}$	2154.11	312.265	0.064	5.05
$E = 34\,168.94\ cm^{-1}$	$4d^35s^2\ a\ {}^4F_{9/2}$	2805.36	318.749	0.248	19.65
$\tau = 10.1 \pm 0.6$	$4d^35s^2\ a\ {}^4P_{5/2}$	5965.45	354.465	0.519	41.13
	$4d^45s\ b\ {}^4F_{9/2}$	13 145.71	475.531	0.027	2.12
	$4d^45s\ b\ {}^4P_{5/2}$	14 899.26	518.805	0.024	1.91
	$4d^45s\ b\ {}^4D_{7/2}$	15 282.35	529.329	0.039	3.11

[a]Deduced from calculated BF values and measured lifetimes obtained in this work.

transition probabilities previously published (Duquette et al. 1986) for 320 lines appearing in the range between 366 and 935 nm.

ACKNOWLEDGMENTS

This work was financially supported by the Integrated Initiative of Infrastructure Project LASERLAB-EUROPE, contract RII3-CT_2003-506350, the Swedish Research Council through the Linnaeus grant, the Knut and Alice Wallenberg Foundation. NSF of Bulgaria is acknowledged for financial support (grant D 02-274/2008). Financial support from the Belgian FRS-FNRS is also acknowledged. ÉB, PQ and PP are Research Directore, Senior Research Associate and Research Associate of this organization, respectively. GM and KB are grateful to the colleagues from the Lund Laser Center for their kind hospitality and support.

REFERENCES

Bergström H., Faris H., Hallstadius G. W., Lundberg H., Persson A., Wahlström C. G., 1988, Z. Phys. D, 8, 17

Corliss C. H., Bozman W. R., 1962, Nat. Bur. Stand. (US), Monogr. 53. Nat. Bur. Stand., US Government Printing Office, Washington DC, USA

Cowan R. D., 1981, The Theory of Atomic Structure and Spectra. University of California Press, Berkeley.

Duquette D. W., Lawler J. E., 1982, Phys. Rev. A, 26, 330
Duquette D. W., Den Hartog E. A., Lawler J. E., 1986, J. Quant. Spectrosc. Radiat. Transfer, 35, 281
Fraga S., Karwowski J., Saxena K. M. S., 1976, Handbook of Atomic Data. Elsevier, Amsterdam
Kröger S., Scharf O., Guthöhrlein G., 2004, Europhys. Lett., 66, 344
Kröger S., Öztürk I. K., Acar F. G., Basar G. C., Basar G., Wyart J.-F., 2007, Eur. Phys. J. D, 41, 61
Kwiatkowski M., Zimmermann P., Biémont É., Grevesse N., 1982, A&A, 112, 337
Moore C. E., 1958, Atomic Energy Levels, Vol. III, Nat. Bur. Stand. Circ. 467. US Government Printing Office, Washington DC, USA
Nilsson H. et al., 2010, A&A, 511, A16
Quinet P., Palmeri P., Biémont E., McCurdy M. M., Rieger G., Pinnington E. H., Wickliffe M. E., Lawler J. E., 1999, MNRAS, 307, 934
Rudolph J., Helbig V., 1982, Phys. Lett. A, 89, 339
Wallerstein G., Dominy J. F., 1986, ApJ, 310, 371

This paper has been typeset from a Microsoft Word file prepared by the author.